

Optimal Planning of a Novel Integrated Renewable Multi-Generation System Based on Biomass Chemical Looping

Du Wen^{a,*}, Muhammad Aziz^b

^aDepartment of Mechanical Engineering, University of Tokyo, 7-3-1 Hongo, Bunkyo-ku, Tokyo 113-8656, Japan

^bInstitute of Industrial Science, University of Tokyo, 4-6-1 Komaba, Meguro-ku, Tokyo 153-8505, Japan
 maziz@iis.u-tokyo.ac.jp

To achieve carbon neutrality in the future, the penetration of renewables requires further improvement with the help of energy storage technology. Green hydrogen and green ammonia have been recognized as the optimal candidate for grid-scale energy storage. Except for water electrolysis, biomass chemical looping technology is another clean hydrogen production method with a cross-sector decarbonization feature. As a result, it starts to attract more concerns. In this study, a novel integrated renewable multi-generation system based on chemical looping technology has been proposed. The technical and economic performance is evaluated after optimal planning. Hydrogen and ammonia are served as energy carriers in two scenarios. The results show that the proposed system is profitable, and the ammonia-based scenario is superior to the hydrogen-based scenario. The cumulative cash position and payback period of the hydrogen-based scenario are 210 MUSD and 12 y, compared to 853 MUSD and 6 y in the ammonia-based scenario.

1. Introduction

When facing global energy issues, e.g., global warming, fossil fuel depletion, and energy security, a green transition of the energy system has been proposed by many countries. To achieve carbon neutrality in the next few decades, inevitably, increasing the penetration of renewables is a significant pathway. However, the intermittent feature of renewables makes it hard to be integrated into the power grid, so energy storage technology has been widely investigated to provide flexibility to the system with high penetration of renewables, even a 100% renewable system. Not all energy storage technologies are suitable for the grid-scale application. Hydrogen storage that uses renewable-driven water electrolysis or other clean production methods to store excess electricity is an important candidate. It characterizes high energy density, large storage capacity, and low self-discharge rate (Aneke and Wang, 2016), contributing to large-scale energy storage. It attracts a lot of concerns in terms of green hydrogen production, storage, and utilization. Except for water electrolysis, biomass chemical looping technology is another carbon-free hydrogen production method with high conversion efficiency and low energy consumption (Fernández and Abanades, 2016). It has a cross-sector decarbonization feature that, unlike traditional steam reforming, avoids using fossil fuels and gathers the carbon in the biomass. If it is powered by renewables, it will be beneficial for reducing carbon emissions in energy (increasing the penetration of renewables), industrial (replacing fossil fuel), and agriculture (clean treatment of biomass) sectors.

The low volumetric density and high hydrogen flammability restrict the utilization of hydrogen storage, considering the cost and safety. Thus, researchers have proposed ammonia to substitute hydrogen because it has high energy density, high hydrogen content, and is a carbon-free fuel compared to other renewable synthesis fuels like methane. Besides, it also has multi-application in fertilizer, refrigerant, synthetic fiber, etc. (Zhang et al., 2020). To better serve as a carbon-free fuel, researchers have investigated its application in fuel cells, gas turbines, and internal combustion engines.

More than energy storage mediums, hydrogen and ammonia are supposed to serve as energy carriers. They are produced when there is excess electricity and consumed for backup power generation when there is an energy shortage. Based on this idea, many studies have proposed different hydrogen- or ammonia-based

energy systems. They mainly focus on techno-economic analysis, optimal planning and sizing, and general system evaluation based on case studies. Less research involves biomass chemical looping technology and makes a comparison between hydrogen and ammonia as energy carriers in energy systems. To offset this gap, in this study, a novel integrated renewable multi-generation system based on chemical looping technology has been proposed. Both hydrogen and ammonia as energy carriers are estimated in two scenarios. The operation of this system is based on optimal planning across a year. After that, the technical and economic performance is evaluated and compared. The novelty of this work is that it conceptualized ammonia as an energy carrier in the renewable multi-generation system based on chemical looping technology. And it makes a comparison of hydrogen and ammonia as energy carriers in the same scale system.

2. Methodology

2.1 System description

The schematic of the novel integrated renewable multi-generation system is shown in Figure 1. It has two subsystems. The power system consists of solar PV, wind turbines, fuel cells, and batteries. The last two of them are served as backup power when there is a lack of electricity. On the contrary, when excess electricity is available, the hydrogen or ammonia production system starts to convert electricity into hydrogen or ammonia. Hydrogen and ammonia are used in fuel cells and sold to the market. The pair of hydrogen or ammonia production systems and fuel cells can be seen as an energy storage method responding to the fluctuant renewables and demand. Only the main components in the hydrogen and ammonia production systems have been shown in the figure, including three in series reactors for the chemical looping process, separators for concentrating resulting gases, heat exchangers for waste heat utilization, and an ammonia synthesis reactor (ASR). The battery is another energy storage method providing more flexibility to the system. System operation is controlled by an energy management system (EMS) which schedules the system according to demand profile, weather forecast, market information, and main objective. The scheduling is based on an optimization problem that focuses on economic or technical goals.

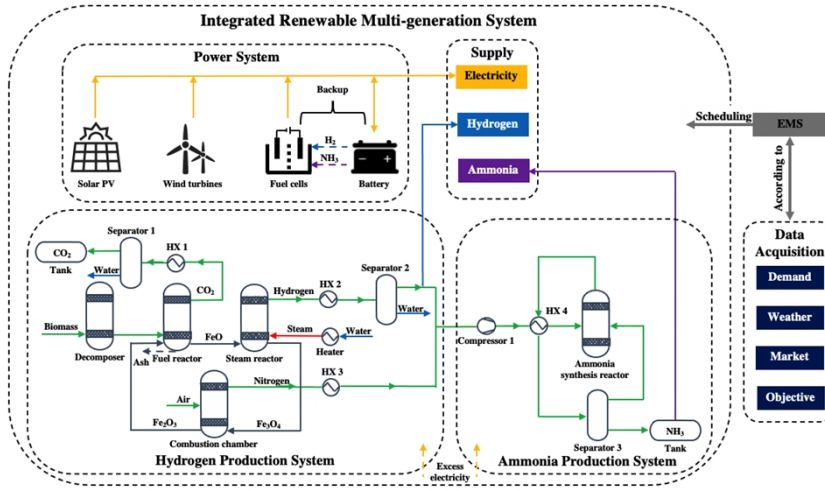


Figure 1: Schematic of the integrated renewable multi-generation system

2.2 Models

Before formulating the optimization problem, the operation of the system should be explicitly expressed. It is assumed that all components in the system work under the ideal condition.

The analytical model of solar PV is used based on reference (Shi et al., 2021):

$$P_{PV} = N_{PV} \eta_{ref} A_{PV} I [1 + \delta(t_c - t_{ref})] \quad (1)$$

$$t_c = \frac{26.6 t_a + I [\tau \alpha - \eta_{ref} (1 - \delta t_{ref})]}{26.6 + \delta \eta_{ref} I} \quad (2)$$

where P_{PV} is the output power of solar PV, [kW]; N_{PV} is the number of solar cells, [-]; η_{ref} is the conversion efficiency of solar cells at a reference temperature, [-]; A_{PV} is the area of a single solar cell, [m²]; I is solar irradiance, [kW · m⁻²]; δ is temperature coefficient, [% · °C⁻¹]; t_c is cell temperature, [°C]; t_{ref} is reference

temperature, [°C]; t_a is ambient temperature [°C]; $\tau\alpha$ is an optical parameter, [-]. The piece-wise power curve of a wind turbine is shown (Lydia et al., 2014):

$$P_{WT} = 0.5N_{WT}\rho A_{WT}C_p v^3 \quad (3)$$

$$v = v_g \left(\frac{h}{h_g} \right)^\beta \quad (4)$$

where P_{WT} is the output power of wind turbines, [kW]; N_{WT} is the number of wind turbines, [-]; ρ is the air density, [$\text{kg}\cdot\text{m}^{-3}$]; A_{WT} is the swept area of a single wind turbine, [m^2]; C_p is power coefficient, [-]; v is wind speed, [$\text{m}\cdot\text{s}^{-1}$]; v_g is measured wind speed near the ground, [$\text{m}\cdot\text{s}^{-1}$]; h is the height of rotor, [m]; h_g is the height of measurement, [m]; β is wind shear exponent, [-].

As for the hydrogen and ammonia production systems, they are simulated in ASPEN Plus V11. The operating parameters in hydrogen production system are chosen from (Steven et al., 2021) and parameters in ammonia production system are chosen from (Khademi and Sabbaghi, 2017). In the simulation, standardized hydrogen and ammonia production systems that have 1 MW input power are achieved and seen as a basic unit. Other inputs and outputs, like utilities and production rate, are bounded to the input power. It is assumed that the system works only under 100 % and 0 % loads. So, in the multi-generation system, the operation of hydrogen and ammonia production systems is represented by the number of available units:

$$m_{\text{H}_2, \text{produced}} = \left\lfloor \frac{P_{\text{allocated}}}{\dot{P}_{\text{std}}} \right\rfloor \dot{m}_{\text{H}_2} \quad (5)$$

where $m_{\text{H}_2, \text{produced}}$ is the produced hydrogen in the multi-generation system, [$\text{kg}\cdot\text{h}^{-1}$]; $P_{\text{allocated}}$ is the allocated power to the hydrogen system, [kW]; \dot{P}_{std} is the rated power of a standardized unit, [kW]; \dot{m}_{H_2} is the produced hydrogen of a standardized unit, [$\text{kg}\cdot\text{h}^{-1}$]. Other inputs and outputs are evaluated by a similar method. It should be noted that there is a loss when the allocated power cannot fulfill the operation of an integer number of units. As for the fuel cell, it uses the same method of evaluating the system inputs and outputs:

$$m_{\text{NH}_3, \text{consumed}} = \left\lceil \frac{P_{\text{allocated}}}{\dot{P}_{\text{std}}} + 1 \right\rceil \dot{m}_{\text{NH}_3} \quad (6)$$

where $m_{\text{NH}_3, \text{consumed}}$ is the consumed ammonia in the multi-generation system, [$\text{kg}\cdot\text{h}^{-1}$]; $P_{\text{allocated}}$ is the allocated power to the ammonia fuel cells, [kW]; \dot{P}_{std} is the rated power of a standardized unit, [kW]; \dot{m}_{NH_3} is the consumed ammonia of a standardized unit, [$\text{kg}\cdot\text{h}^{-1}$]. The difference is that the backup power should be larger than the shortage.

The state of battery is denoted by stored energy and state of charge (SoC) (Aaslid et al., 2020):

$$E_t = E_{t-1} + \eta_c P_c = E_{t-1} - \frac{P_d}{\eta_d} \quad (7)$$

$$\text{SoC}_t = \text{SoC}_{t-1} \pm \frac{I\Delta t}{\text{SoC}_{\text{max}}} \quad (8)$$

where E_t is the stored energy at time t , [kWh]; η_c is charging efficiency, [-]; P_c is charging power, [kW]; η_d is discharging efficiency, [-]; P_d is discharging power, [kW]; SoC_t is the state of charge at time t , [Ah]; SoC_{max} is the maximum storage capacity of batteries, [Ah].

The profitability is denoted by the cumulative cash position (CCP) and payback period:

$$\text{CCP} = \left(\sum_{j=1}^n \left(\frac{(C_{\text{rev}} - \text{OPEX} - d_j) \times (1 - t) + d_j}{(1 + i)^j} \right) - \text{CAPEX} \right) \quad (9)$$

where n is system lifetime; C_{rev} is annual revenue; OPEX is operational expenditure (OPEX); t is tax rate; d_j is annual depreciation cost. i is annual interest rate; CAPEX is capital expenditure (CAPEX). The payback period is the year CCP becomes positive. The profitability is influenced by CAPEX and OPEX:

$$\text{CAPEX}_i = \text{CAPEX}_b \left(\frac{A_i}{A_b} \right)^n \quad (10)$$

$$OPEX = C_{RM} + C_{UT} + C_{WT} + C_{OL} + C_{IM} \quad (11)$$

where CAPEX_{*i*} is the CAPEX of component *i*; *A_i* is the equipment cost attribute of component *i*; CAPEX_{*b*} is the CAPEX of a component on the baseline condition in the reference; *n* is the cost exponent; *C_{RM}* is the cost of raw material; *C_{UT}* is the cost of utility; *C_{WT}* is the cost of waste treatment; *C_{OL}* is the cost of operating labor; *C_{IM}* is the cost of insurance and maintenance. The references for CAPEX and OPEX estimation are shown in Table 1. The estimation of other components, like compressors, is conducted based on (Turton et al., 2008). The utility prices like cooling water are taken from (Turton et al., 2008) as well.

Table 1: References for CAPEX and OPEX estimation

Name	Value	Name	Value	Name	Value
Solar PV	1,340 USD/kW	System lifetime	25 y	Biomass price	60 USD/t
Wind turbine	1,514 USD/kW	Hydrogen price	1,500 USD/t	Catalyst (ASR)	20 USD/kg
Battery	236 USD/kW	Ammonia price	514 USD/t	Oxygen carrier (CL)	20 USD/kg
Membrane	10,764 USD/m ²	Carbon dioxide price	30 USD/t		

2.3 Problem formulation

The optimal planning of the system is described as a mixed-integer linear programming problem where the objective function is:

$$\max(C_{rev,t} - OPEX_t) \quad (12)$$

It is expected to maximize the revenue in each time interval. The problem is solved by a commercial solver Gurobi. The objective function is restricted by energy and mass balance (Equations 13 and 14, respectively).

$$P_d + P_{cur} = P_{solar} + P_{wind} \pm P_{battery} - P_{hydrogen} + P_{fuel\ cell} + P_{grid} \quad (13)$$

$$m_{H_2,sto}^t = m_{H_2,sto}^{t-1} + m_{H_2,CL}^t - m_{H_2,FC}^t - m_{H_2,loss}^t - m_{H_2,sold}^t \quad (14)$$

where *P_d* is demand; *P_{cur}* is curtailment; *P_{battery}* is charge or discharge power of battery; *P_{hydrogen}* is the input power of hydrogen production; *P_{fuel cell}* is the output power of fuel cells; *P_{grid}* is import electricity from the grid; *m_{H₂,sto}^t* is the amount of hydrogen stored at time *t*; *m_{H₂,CL}^t* is the produced hydrogen by chemical looping; *m_{H₂,FC}^t* is the consumed hydrogen by fuel cells; *m_{H₂,loss}^t* is the losses during operation; *m_{H₂,sold}^t* is the amount of sold hydrogen. The energy and mass balance of the ammonia-based system is the same.

2.4 Input data

The weather information, including net solar irradiance, wind speed, and ambient temperature, is obtained from MERRA-2 database (Global Modeling and Assimilation Office (GMAO), 2015), while the demand profile and day-ahead electricity price are taken from the Renewable Energy Institute of Japan.

3. Results and discussion

In this study, the novel integrated renewable multi-generation system is evaluated based on optimal planning. Two energy carriers, hydrogen and ammonia, are compared with respect to technical and economic aspects in scenarios S1 (hydrogen-based) and S2 (ammonia-based).

3.1 Technical performance

The yearly distribution of the state of charge in scenarios S1 and S2 is shown in Figure 2.

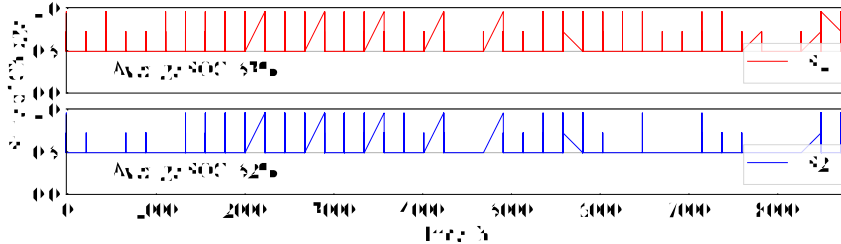


Figure 2: Yearly distribution of the state of charge in scenarios S1 and S2

It is clear that they have similar distribution characteristics with an average SoC of 52 % - 53 %. Because with the same input power selling the produced hydrogen and ammonia is more beneficial than directly selling electricity, the hydrogen or ammonia storage is prior to battery storage. Only when the excess electricity is larger than the rated power of the hydrogen or ammonia production system, the battery starts to be charged. And it is first used when there is an electricity shortage. Thus, the battery is less involved in the operation under the current configuration.

The monthly distribution of hydrogen and ammonia production is shown in Figure 3. Due to the priority, hydrogen and ammonia production is fulfilled at first, so the production rates of hydrogen and ammonia each month are similar, around 5,000 t and 25,000 t. The decreases in August and September are caused by a demand surge, while the decrease in December is due to the lack of renewables.

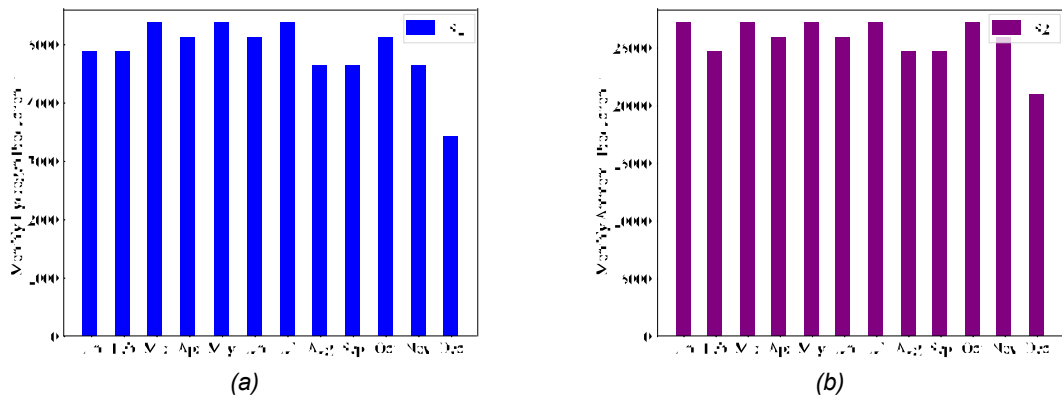


Figure 3: Monthly distribution of net hydrogen (a) and ammonia (b) production

3.2 Economic performance

The breakdown of CAPEX of hydrogen- and ammonia-based systems is shown in Figure 4. The total CAPEX is 239 MUSD and 317.7 MUSD. They have the same investment in solar (PV), wind (WT), biomass chemical looping (BCL) hydrogen production, and battery (B), which are 27.43 MUSD, 41.64 MUSD, 119.31 MUSD, and 9.33 MUSD, respectively. The main difference is presented in the extra ammonia synthesis (AS) system, which causes an extra 99.88 MUSD and the cost of hydrogen storage (24.42 MUSD) is higher than that of ammonia storage (3.3 MUSD).

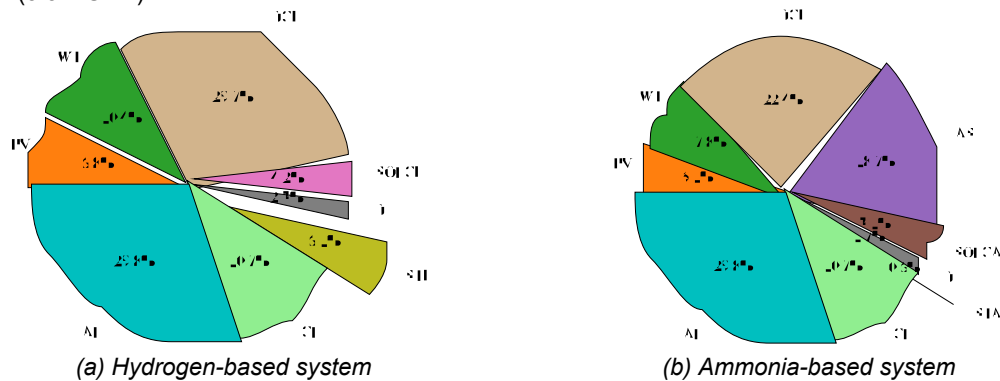


Figure 4: Breakdown of CAPEX

The breakdown of OPEX and revenues of scenarios S1 and S2 are shown in Figure 5. The main part of OPEX is from the costs of raw material (biomass) and utility (except for electricity). Electricity is supposed to earn money but becomes cost in both scenarios. Because compared to water electrolysis unit input power can produce more hydrogen in the BCL system with the higher cost of raw material and utility. That cost is easily covered by selling hydrogen or ammonia, so EMS prioritizes to satisfy the operation of BCL under the full load condition, which causes the relatively higher cost of electricity. Besides, the ammonia-based system has an extra cost of a waste treatment since ammonia is noxious. As for revenues, selling hydrogen and ammonia earns 87 MUSD and 156.6 MUSD, while selling carbon dioxide gains 27.5 - 28.5 MUSD. The higher revenue of ammonia is caused by the higher production rate of ammonia which is fivefold the production rate of hydrogen. It is clear that using ammonia as an energy carrier causes 30 MUSD more OPEX, but revenue accordingly

increases by 70 MUSD. The profitability of the two scenarios is shown in Table 2. With a similar configuration (at the same scale), the ammonia-based system (S2) is superior to the hydrogen-based system (S1). The CCP is 853 MUSD against 210 MUSD, while PBP is 6 y against 12 y.

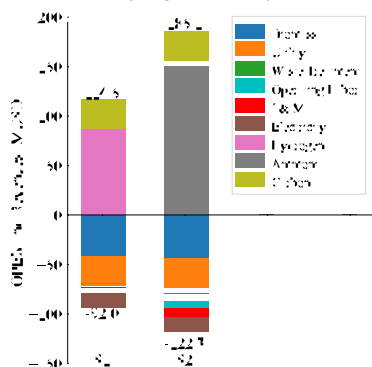


Figure 5: Breakdown of OPEX in scenarios S1 (a) and S2 (b)

Table 2: Cumulative cash position and payback period of scenarios S1 and S2

Name	Solar PV	Wind turbine	Hydrogen production	Ammonia production	Fuel cell	Battery	CCP	PBP
S1	20 MW	30 MW	15 MW	-	15 MW	20 MWh	210 MUSD	12 y
S2	20 MW	30 MW	-	15 MW	15 MW	20 MWh	853 MUSD	6 y

4. Conclusions

This study proposes a novel integrated renewable multi-generation system and technically and economically evaluates its performance. The results show that the system shows acceptable profitability. The CCP of hydrogen- and ammonia-based scenarios is 210 MUSD and 853 MUSD, while the relevant PBP are 12 y and 6 y. The higher production rate of ammonia makes the ammonia-based system superior to the hydrogen-based system, although it has more CAPEX and OPEX. Future work will be conducted on the multi-objective optimization of the system regarding both scheduling and sizing.

References

- Aaslid P., Geth F., Korpås M., Belsnes M.M., Fosso O.B., 2020, Non-linear charge-based battery storage optimization model with bi-variate cubic spline constraints, *Journal of Energy Storage*, 32, 101979.
- Aneke M., Wang M., 2016, Energy storage technologies and real life applications – A state of the art review, *Applied Energy*, 179, 350-377.
- Fernández J., Abanades J., 2016, Novel Process for Hydrogen Production Through the Sorption Enhanced Reforming of Methane Combined with Chemical Looping Combustion, *Chemical Engineering Transactions*, 52, 535-540.
- Global Modelling and Assimilation Office (GMAO), 2015, MERRA-2 tavg1_2d_rad_Nx: 2d,1-Hourly,Time-Averaged,Single-Level,Assimilation,Radiation Diagnostics V5.12.4, Greenbelt, MD, USA, Goddard Earth Sciences Data and Information Services Center (GES DISC). https://disc.gsfc.nasa.gov/datasets/M2T1NXRAD_5.12.4/summary (accessed 15.04.2022).
- Khademi M.H., Sabbaghi R.S., 2017, Comparison between three types of ammonia synthesis reactor configurations in terms of cooling methods, *Chemical Engineering Research and Design*, 128, 306-317.
- Lydia M., Kumar S.S., Selvakumar A.I., Prem Kumar G.E., 2014, A comprehensive review on wind turbine power curve modeling techniques, *Renewable and Sustainable Energy Reviews*, 30, 452-460.
- Shi Y., Sun Y., Liu J., Du X., 2021, Model and stability analysis of grid-connected PV system considering the variation of solar irradiance and cell temperature, *International Journal of Electrical Power & Energy Systems*, 132, 107155.
- Steven S., Restiawaty E., Bindar Y., 2021, Routes for energy and bio-silica production from rice husk: A comprehensive review and emerging prospect, *Renewable and Sustainable Energy Reviews*, 149, 111329.
- Turton R., Bailie R.C., Whiting W.B., Shaiwitz J.A., 2008, Analysis, synthesis, and design of chemical processes, 3ed, Pearson Education, the United States of America.
- Zhang H., Wang L., Van Herle J., Maréchal F., Desideri U., 2020, Techno-economic comparison of green ammonia production processes, *Applied Energy*, 259, 114135.